

Quark Mass Textures and $\sin 2\beta$

Hyung Do Kim^{a,b}, Stuart Raby^a and Leslie Schradin^a

*^aDepartment of Physics, The Ohio State University,
174 W. 18th Ave., Columbus, Ohio 43210, USA*

*^bSchool of Physics, Seoul National University,
Seoul, 151-747, Korea*

E-mail: hdkim,raby,schradin@mps.ohio-state.edu

ABSTRACT: Recent precise measurements of $\sin 2\beta$ from the B-factories (BABAR and BELLE) and a better known strange quark mass from lattice QCD make precision tests of predictive texture models possible. The models tested include those hierarchical N-zero textures classified by Ramond, Roberts and Ross, as well as any other hierarchical matrix Ansatz with non-zero $12 = 21$ and vanishing 11 and 13 elements. We calculate the maximally allowed value for $\sin 2\beta$ in these models and show that all the aforementioned models with vanishing 11 and 13 elements are ruled out at the 3σ level. While at present $\sin 2\beta$ and $|V_{ub}/V_{cb}|$ are equally good for testing N-zero texture models, in the near future the former will surpass the latter in constraining power.

KEYWORDS: Quark Mass, Mixing Angles, CP Violation, Texture Zeros.

Contents

1. Introduction	1
2. Data	3
2.1 CKM elements	3
2.2 Masses	3
3. Setup	4
4. Analysis	7
4.1 2×2 light quark matrices	7
4.2 3×3 quark matrices	7
4.2.1 Models with $11 = 13 = 0$ and $12 = 21 \neq 0$	8
4.2.2 Models with non-zero 13 elements	11
5. Conclusion	12
A. Loop Rephasing Method	13

1. Introduction

The problem of understanding the origin of fermion masses has persisted for more than twenty years [1, 2, 3]. Models predicting relations between fermion masses and mixing angles may give insights into possible solutions to this problem. On the other hand, testing theories of fermion masses requires precision data; the accuracy of which has been severely limited by theoretical uncertainties inherent in QCD. In particular, light quark masses and some CKM elements have been difficult to measure with precision. Recent results from B-factories combined with advances in the theory of heavy quarks as well as in lattice QCD have reduced the errors considerably for these observables [4, 5]. Current measurements of $|V_{us}|$ and $|V_{cb}|$ have errors at the 2% level [4]. $\sin 2\beta$ is now known to 6.5% from experiments on the asymmetry in B decays [5]. Even $|V_{ub}/V_{cb}|$, whose errors largely come from non-perturbative QCD effects, has now been determined to about 10% [4]. In the mass sector, the most important improvement has been in m_s ,

whose uncertainty has decreased from 50% to 12% over the last ten years. Moreover, lattice QCD results with light dynamical quarks indicate that the strange quark mass is much lighter than previously thought [6].

In a pioneering work Hall and Rasin [7] showed that the relation

$$|V_{ub}/V_{cb}| = \sqrt{m_u/m_c} \quad (1.1)$$

is obtained for any hierarchical texture with vanishing 11, 13, 31 elements. Roberts et al. [8] then re-analyzed these textures, using more recent data, and concluded that such textures were disfavored, i.e. disagreeing with data at about 1σ (see also [9]). Whereas the addition of a small $13 \approx 31$ element gave good fits to the data. They also studied non-hierarchical asymmetric textures, with vanishing 13, 31 elements but satisfying the “lopsided” relation $32 \sim 33$. Good fits to the data were also obtained in this case. The strongest constraint, in their analysis, came from the observable $|V_{ub}/V_{cb}|$, which at the time had an uncertainty $\mathcal{O}(22\%)$.¹ On the other hand, the value of $\sin 2\beta$ was not well known and, in fact, the central value was much lower than it is now. However, with symmetric textures with non-zero $13 = 31$ elements, they predicted $\sin 2\beta$ to be near its present experimental value.

With the significant improvement in the data, we feel that it is once again a good time to re-analyze quark mass textures. In this paper we study hierarchical textures satisfying $12 = 21$. We find that such textures, with vanishing 11, 13, 31 elements, are now excluded by 3σ . In the present study, constraints from both $|V_{ub}/V_{cb}|$ and $\sin 2\beta$ are equally strong. However, in the near future $\sin 2\beta$ may provide the most stringent constraint. For example, it is expected that the experimental precision of $\sin 2\beta$ will greatly improve (by a factor of 2), perhaps by 2006 when an expected 500 fb^{-1} of data will have been tabulated by both BaBar and Belle [10]. On the other hand, the experimental uncertainties associated with $|V_{ub}/V_{cb}|$ (limited by uncertainties in $|V_{ub}|$) may require a Super-B factory (perhaps by 2010 [11]) to obtain a similar factor of 2 reduction [12].

In Section 2 we tabulate the latest data on quark masses and mixing angles. Then in Section 3 we present the relevant approximations used when diagonalizing hierarchical fermion mass textures. In Section 4.1, as a warm-up, we consider the oldest successful texture describing the lightest two quark families. We then obtain our main result in Section 4.2.1 where we study hierarchical 3×3 quark mass textures satisfying $12 = 21$ with $11 = 13 = 31 \equiv 0$. Finally in Section 4.2.2 we show that good fits to the data can be obtained with non zero 13, 31 elements. In particular we focus on two 5-zero texture models considered by Ramond et al. [13].

¹Although Roberts et al. assumed an uncertainty half this size [8].

2. Data

In this Section we tabulate the present data for CKM elements and quark masses used in our analysis.

2.1 CKM elements

We take the CKM element values from [4] and $\sin 2\beta$ from [5].

$$\begin{aligned}
 |V_{us}| &= 0.2240 \pm 0.0036 \\
 |V_{cb}| &= (41.5 \pm 0.8) \times 10^{-3} \\
 |V_{ub}| &= (35.7 \pm 3.1) \times 10^{-4} \\
 \left| \frac{V_{ub}}{V_{cb}} \right| &= 0.086 \pm 0.008 \\
 \sin 2\beta &= 0.739 \pm 0.048
 \end{aligned} \tag{2.1}$$

The errors on $\sin 2\beta$ are mostly statistical while those on $\left| \frac{V_{ub}}{V_{cb}} \right|$ are largely theoretical. As more data is taken, $\sin 2\beta$ will become more precisely known, but the precision in $\left| \frac{V_{ub}}{V_{cb}} \right|$ will likely remain at the 10% level for some time.

2.2 Masses

Due to strong interactions, the masses of the light quarks are not known well. The most precise estimates of m_u/m_d and m_s/m_d come from chiral perturbation theory. There is some disagreement in the literature on the sizes of the errors of the light quark mass ratios [14]. For this reason, we take m_u/m_d and m_s/m_d from [15] with doubled errors.

Recent lattice QCD calculations with dynamical quarks have improved our knowledge of m_s , previously the least known of the light quarks. We use the unquenched lattice QCD result with $n_f = 2$ for m_s [6] and double the error to account for the discrepancy with the sum rule result. The central value (Eqn. 2.2) is near the low end of the range given by the PDG [14]. The preliminary result with $n_f = 2 + 1$ indicates that the strange quark might be even lighter.

For the charm quark mass we use a quenched lattice QCD result since an unquenched calculation is not yet available. Quenching errors are known to be about 25% for the strange quark mass and 1 to 2% for the bottom quark mass. Because of the mass hierarchy, it is expected that the quenching error on m_c will lie somewhere between these two bounds. Thus we take the lattice QCD result with a (probably conservative) 10 percent systematic (quenching) error as in [4] and double it.

We use the bottom quark mass from [16] and the top quark pole mass from the Particle Data Group (PDG) 2003 [14].

$$\begin{aligned}
\frac{m_u}{m_d} &= 0.553 \pm 0.043 \times 2 \\
\frac{m_s}{m_d} &= 18.9 \pm 0.8 \times 2 \\
m_s(2 \text{ GeV}) &= 89 \pm 11 \times 2 \text{ MeV} \\
m_c(m_c) &= 1.30 \pm 0.15 \times 2 \text{ GeV} \\
m_b(m_b) &= 4.22 \pm 0.09 \text{ GeV}. \\
M_t(\text{pole}) &= 174.3 \pm 5.1 \text{ GeV} \\
m_t(m_t) &= 165 \pm 5 \text{ GeV}
\end{aligned} \tag{2.2}$$

All running mass parameters are defined in the $\overline{\text{MS}}$ scheme. We note here that the doubled errors we are using almost incorporate the bounds found in the PDG [14].

For the purposes of further analysis we compare to fermion masses evaluated at M_Z . We define the renormalization factor

$$\eta_i \equiv \begin{cases} \frac{m_i(M_Z)}{m_i(m_i)} & \text{for } i = c, b, t \\ \frac{m_i(M_Z)}{m_i(2 \text{ GeV})} & \text{for } i = u, d, s. \end{cases} \tag{2.3}$$

At two loops in QCD we find

$$\begin{aligned}
\eta_c &= 0.56, & \eta_b &= 0.69, & \eta_t &= 1.06 \\
\eta_u &= \eta_d = \eta_s = 0.65.
\end{aligned} \tag{2.4}$$

3. Setup

This section introduces our notation for the Yukawa and CKM matrices. Quark masses are expressed in terms of Weyl spinors as

$$-\mathcal{L} = Q_i Y_{ij}^U \langle H_u \rangle u_j^c + Q_i Y_{ij}^D \langle H_d \rangle d_j^c, \tag{3.1}$$

where $i, j = 1, 2, 3$ are the family indices, $Q = \begin{pmatrix} u \\ d \end{pmatrix}$ is the left-handed quark doublet, u^c and d^c are the left-handed anti-up and -down quarks, and H_u and H_d are the up and down Higgs fields. To keep track of phases in Y^U and Y^D , which in general are complex, we define $\phi_{ij}^U \equiv \arg Y_{ij}^U$ and $\phi_{ij}^D \equiv \arg Y_{ij}^D$. Two unitary matrices V_U and U_{U^c} diagonalize the up quark Yukawa matrix by

$$V_U Y^U U_{U^c} = Y_{\text{Diag}}^U.$$

Similarly, V_D and U_{D^c} diagonalize Y^D . We assume that the mass matrices are hierarchical [7] which means

$$\begin{aligned} \left| \frac{Y_{(23,32)}^{(U,D)}}{Y_{33}^{(U,D)}} \right| &\ll 1, & \left| \frac{\tilde{Y}_{22}^{(U,D)}}{Y_{33}^{(U,D)}} \right| &\ll 1, \\ \left| \frac{Y_{(12,21)}^{(U,D)}}{\tilde{Y}_{22}^{(U,D)}} \right| &\ll 1, & \left| \frac{Y_{11}^{(U,D)}}{\tilde{Y}_{22}^{(U,D)}} \right| &\ll 1, \\ \left| \frac{Y_{13}^{(U,D)} Y_{31}^{(U,D)}}{Y_{33}^{(U,D)}} \right| &\ll \left| \frac{Y_{12}^{(U,D)} Y_{21}^{(U,D)}}{\tilde{Y}_{22}^{(U,D)}} \right|, \end{aligned} \quad (3.2)$$

where

$$\tilde{Y}_{22} \equiv Y_{22} - \frac{Y_{23} Y_{32}}{Y_{33}} \equiv \left| \tilde{Y}_{22} \right| e^{i\tilde{\phi}_{22}} \quad (3.3)$$

is used since we will consider both of the following cases:

$$0 = |Y_{22}| < \left| \frac{Y_{23} Y_{32}}{Y_{33}} \right| \quad \text{and} \quad 0 \neq |Y_{22}| \gtrsim \left| \frac{Y_{23} Y_{32}}{Y_{33}} \right|. \quad (3.4)$$

Note, an approximately symmetric matrix ansatz will be hierarchical unless the known CKM mixing angles come as a surprising cancellation of two large angles for up and down quarks. We also note that there are “lopsided” textures in the literature with $|Y_{32}| \sim |Y_{33}|$ which do not fulfill the conditions described above. We do not consider such asymmetric textures in this paper. For an analysis of these models, see [8].

With no order one off-diagonal terms in Y^U or Y^D , we can neglect higher powers of the mixing angles and keep $\cos \theta \simeq 1$. This makes the mixing matrices quite simple.

$$V_U = \begin{pmatrix} 1 & -s_{12}^U & 0 \\ s_{12}^{U*} & 1 & 0 \\ 0 & 0 & 1 \end{pmatrix} \begin{pmatrix} 1 & 0 & -s_{13}^U \\ 0 & 1 & 0 \\ s_{13}^{U*} & 0 & 1 \end{pmatrix} \begin{pmatrix} 1 & 0 & 0 \\ 0 & 1 & -s_{23}^U \\ 0 & s_{23}^{U*} & 1 \end{pmatrix}. \quad (3.5)$$

V_D has the same form. The s_{ij}^U can be considered as generalized mixing angles carrying both a real mixing angle and a phase.

The CKM matrix $V_{CKM} = V_U^* V_D^T$ is then given by

$$V_{CKM} = \begin{pmatrix} 1 & s_{12}^* + s_{13}^{U*} s_{23} & -s_{12}^{U*} s_{23}^* + s_{13}^* \\ -s_{12} - s_{13}^D s_{23}^* & 1 & s_{23}^* + s_{12}^U s_{13}^* \\ s_{12}^D s_{23} - s_{13} & -s_{23} - s_{12}^D s_{13} & 1 \end{pmatrix}, \quad (3.6)$$

where

$$\begin{aligned}
s_{12}^U &\simeq \frac{Y_{12}^U}{\tilde{Y}_{22}^U}, & s_{12}^D &\simeq \frac{Y_{12}^D}{\tilde{Y}_{22}^D}, \\
s_{13}^U &\simeq \frac{Y_{13}^U}{Y_{33}^U}, & s_{13}^D &\simeq \frac{Y_{13}^D}{Y_{33}^D}, \\
s_{23}^U &\simeq \frac{Y_{23}^U}{Y_{33}^U}, & s_{23}^D &\simeq \frac{Y_{23}^D}{Y_{33}^D}, \\
s_{23} &\equiv s_{23}^D - s_{23}^U, & s_{12} &\equiv s_{12}^D - s_{12}^U, & s_{13} &\equiv s_{13}^D - s_{13}^U.
\end{aligned} \tag{3.7}$$

The above approximations work well, *except* in the case of first and second generation mixing. For $|Y_{11}^D| = 0$, $|Y_{12}^D| = |Y_{21}^D|$, which we will address in this paper, $|s_{12}^D| = \left| \frac{Y_{12}^D}{\tilde{Y}_{22}^D} \right| \simeq \sqrt{\frac{m_d}{m_s}} \left(1 + \mathcal{O}\left(\frac{m_d}{m_s}\right) \right)$. To capture the rather large $\mathcal{O}\left(\frac{m_d}{m_s}\right) \sim 5\%$ correction properly, we must include at least through $\mathcal{O}(|s_{12}^D|^2)$ in $c_{12}^D \equiv \sqrt{1 - |s_{12}^D|^2}$. We need do this only for the first and second generation mixing in the down sector, for all other mixing angles are small enough that the errors from our approximations are below 1%. (e.g., $\frac{m_u}{m_c} \sim 2 \times 10^{-3}$).

An exact diagonalization of the 2×2 submatrix for down quarks gives

$$|s_{12}^D| = \sqrt{\frac{m_d}{m_s + m_d}} \tag{3.8}$$

and thus $|s_{12}|$ ($\subset |V_{us}|$) is given by,²

$$|s_{12}| = \sqrt{\frac{m_s}{m_s + m_d}} \left| \sqrt{\frac{m_d}{m_s}} - e^{i\phi} \sqrt{\frac{m_u}{m_c}} \right| \tag{3.9}$$

where $\phi \equiv (\phi_{12}^U - \tilde{\phi}_{22}^U) - (\phi_{12}^D - \tilde{\phi}_{22}^D)$. For $Y_{12}^U = Y_{21}^U = 0$ we have

$$|s_{12}| = \sqrt{\frac{m_d}{m_s + m_d}}. \tag{3.10}$$

Furthermore, $|s_{23}| \sim 0.04 \ll |s_{12}|$ and we have $V_{us} = s_{12}^* + s_{13}^{U*} s_{23} \simeq s_{12}^*$ within a 1% error. Therefore, $V_{us} = s_{12}^*$ is used.

We will also need β , the most precisely measured angle within the unitarity triangle. In terms of CKM matrix elements:

$$\beta = \arg \left(-\frac{V_{cd} V_{cb}^*}{V_{td} V_{tb}^*} \right). \tag{3.11}$$

²In Eqn. 3.9 the second factor includes the cosine of the down quark mixing angle, i.e. $s_{12}^U \rightarrow s_{12}^U c_{12}^D$.

4. Analysis

In this section we confront the data. We first consider the 2×2 subsector of light quarks and show that good fits to the data are obtained. In section 4.2 we extend the analysis to the full 3×3 case.

4.1 2×2 light quark matrices

The Cabbibo angle, in the original texture by Weinberg [1], is generated solely by the down quark Yukawa matrix. The Yukawa matrices are given by

$$Y^U = \begin{pmatrix} A & 0 \\ 0 & B \end{pmatrix} \quad Y^D = \begin{pmatrix} 0 & C \\ C & D \end{pmatrix} \quad (4.1)$$

where the parameters A , B , C , D can be taken to be real without loss of generality. Hence

$$|V_{us}| = \sqrt{\frac{m_d}{m_s + m_d}} \quad (4.2)$$

which works surprisingly well since the observed $|V_{us}| = 0.2240 \pm 0.0036$ is just the same as $\sqrt{\frac{m_d}{m_s + m_d}} = 0.224 \pm 0.004$.

On the other hand, if Y^U is taken to have the same form as Y^D then a non-removable phase enters in the determination of $|V_{us}|$. We then find

$$|V_{us}| = \sqrt{\frac{m_s}{m_s + m_d}} \left| \sqrt{\frac{m_d}{m_s}} - e^{i\phi} \sqrt{\frac{m_u}{m_c}} \right|. \quad (4.3)$$

Note, using the central value of the quark masses, V_{us} has the right value for $\phi \sim \frac{\pi}{2}$. However, due to the large uncertainties in the light quark masses, the value of ϕ is not significantly constrained.

In what follows, we always assume $|Y_{12}^D| = |Y_{21}^D| \neq 0$ and $Y_{11}^{(U,D)} = 0$. These conditions imply that $|V_{us}|$ is given by either equation (4.2) or (4.3). We will be using these expressions for $|V_{us}|$ throughout the rest of the analysis.

4.2 3×3 quark matrices

Over the next two subsections we address two categories of 3 generation quark textures. In section 4.2.1, we consider textures with zero 11 and 13 elements and symmetric 12 and 21 elements. We show that all such textures, provided they are hierarchical, are ruled out. These include the 5-zero models I, II, and IV, nominally consistent with previous data, classified by Ramond et. al. in [13] and listed in Table 1.³ Section 4.2.2

³6-zero symmetric texture models are already ruled out [13].

Table 1: The symmetric 5-zero textures classified in [13]. The number of zeros (here, 5) refers to the total number of zero elements in the upper-right and diagonal portions of the up and down matrices.

	Y^U	Y^D
I	$\begin{pmatrix} 0 & X & 0 \\ X & X & 0 \\ 0 & 0 & X \end{pmatrix}$	$\begin{pmatrix} 0 & X & 0 \\ X & X & X \\ 0 & X & X \end{pmatrix}$
II	$\begin{pmatrix} 0 & X & 0 \\ X & 0 & X \\ 0 & X & X \end{pmatrix}$	$\begin{pmatrix} 0 & X & 0 \\ X & X & X \\ 0 & X & X \end{pmatrix}$
III	$\begin{pmatrix} 0 & 0 & X \\ 0 & X & 0 \\ X & 0 & X \end{pmatrix}$	$\begin{pmatrix} 0 & X & 0 \\ X & X & X \\ 0 & X & X \end{pmatrix}$
IV	$\begin{pmatrix} 0 & X & 0 \\ X & X & X \\ 0 & X & X \end{pmatrix}$	$\begin{pmatrix} 0 & X & 0 \\ X & X & 0 \\ 0 & 0 & X \end{pmatrix}$
V	$\begin{pmatrix} 0 & 0 & X \\ 0 & X & X \\ X & X & X \end{pmatrix}$	$\begin{pmatrix} 0 & X & 0 \\ X & X & 0 \\ 0 & 0 & X \end{pmatrix}$

covers textures with non-zero 13 elements. We choose to study models III and V of Table 1, the most constrained of these models, to illustrate that texture models of this type with 5 or fewer zeros are consistent with the data.

4.2.1 Models with $11 = 13 = 0$ and $12 = 21 \neq 0$

We consider here hierarchical texture models with $Y_{11}^{(U,D)} = Y_{13}^{(U,D)} = 0$, $|Y_{12}^U| = |Y_{21}^U| \neq 0$, and $|Y_{12}^D| = |Y_{21}^D| \neq 0$ which include type I, II and IV of [13]. By the method presented in the Appendix, we see that there are 2 non-removable phases in the mass matrices for I and IV and 3 phases are non-removable for II.⁴ The location of these phases can be chosen as follows:

I	ϕ_{22}^D	ϕ_{22}^U	
II	ϕ_{22}^D	ϕ_{23}^U	ϕ_{32}^U
IV	ϕ_{22}^D	ϕ_{32}^U	

⁴Note, in our analysis we specifically use the phases from I, II and IV 5-zero models. Nevertheless, since we are interested in $|V_{ub}/V_{cb}|$ and in the maximum value for $\sin 2\beta$ our results hold for all models with $13 = 31 = 0$ and $12 = 21 \neq 0$.

$Y_{13}^U = Y_{13}^D = 0$ implies $s_{13} = 0$, and the CKM matrix becomes extremely simple:

$$V_{CKM} = \begin{pmatrix} 1 & s_{12}^* & -s_{12}^{U*} s_{23}^* \\ -s_{12} & 1 & s_{23}^* \\ s_{12}^D s_{23} & -s_{23} & 1 \end{pmatrix} \quad (4.4)$$

$$s_{12}^U = \frac{Y_{12}^U}{\bar{Y}_{22}^U} \simeq \sqrt{\frac{m_u}{m_c}} e^{-i\tilde{\phi}_{22}^U} \quad (4.5)$$

$$s_{12}^D \simeq \sqrt{\frac{m_d}{m_s + m_d}} e^{-i\tilde{\phi}_{22}^D}$$

$$\tilde{\phi}_{22} \equiv \tilde{\phi}_{22}^D - \tilde{\phi}_{22}^U.$$

We now use these angles to find the CKM elements and β in terms of mass ratios and phases. In the case of $|V_{us}|$, we use the expression found in equation (4.3) (also see footnote ² with regards to β).

$$|V_{us}| = \sqrt{\frac{m_s}{m_s + m_d}} \left| \sqrt{\frac{m_d}{m_s}} - e^{-i\tilde{\phi}_{22}} \sqrt{\frac{m_u}{m_c}} \right| \quad (4.6)$$

$$\left| \frac{V_{ub}}{V_{cb}} \right| = |s_{12}^U| \simeq \sqrt{\frac{m_u}{m_c}}$$

$$\beta = \arg\left(\frac{s_{12}}{s_{12}^D}\right) = \arg\left(1 - \frac{s_{12}^U c_{12}^D}{s_{12}^D}\right) \simeq \arg\left(1 - r e^{i\tilde{\phi}_{22}}\right)$$

where

$$r \equiv \sqrt{\frac{m_u}{m_c} \frac{m_s}{m_d}}. \quad (4.7)$$

Since $r \sim 1/4 \ll 1$, β is restricted to be a small angle. The maximum value for β , i.e. β_{\max} , is given by

$$\begin{aligned} \sin \beta_{\max} &= r, \\ \sin 2\beta_{\max} &= 2r\sqrt{1 - r^2}. \end{aligned} \quad (4.8)$$

Using the data for the quark masses, we get $r = 0.22 \pm 0.04$. Thus this texture model results in

$$\sin 2\beta_{\max} = 0.43 \pm 0.08. \quad (4.9)$$

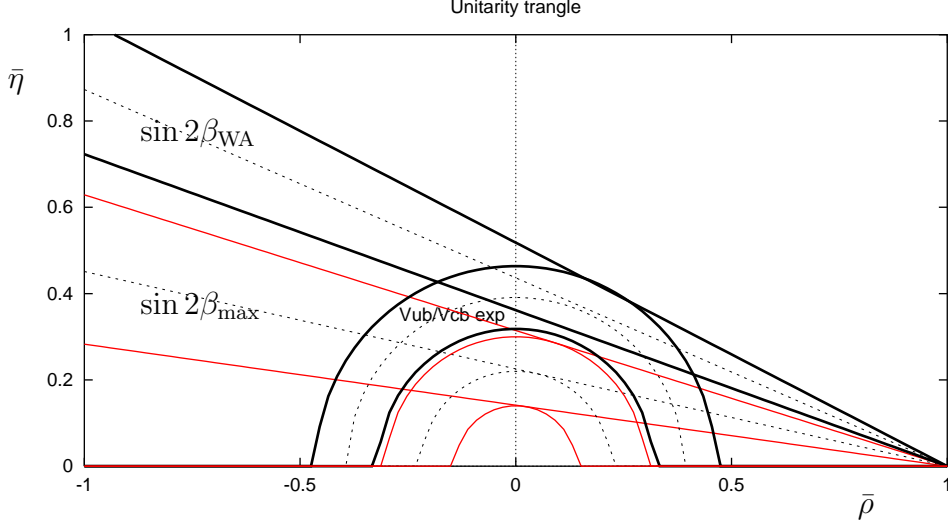


Figure 1: Comparisons between experiment and predictions of hierarchical $11 = 13 = 0$ and $12 = 21$ models. Shown are the 2σ lines for the predicted $\sin 2\beta_{\max}$ (in red or grey) and the measured $\sin 2\beta$ (in black). The red (or grey) arcs correspond to the 2σ range of the predicted $|V_{ub}/V_{cb}|$, while the black arcs show the 2σ range of the experimental value. The dotted lines and arcs are the corresponding central values. There is no overlap between the predictions and experiment for either observable.

Given the world average $\sin 2\beta_{\text{WA}} = 0.739 \pm 0.048$, this texture is ruled out by at least 3.4σ .⁵ Using equation (4.6), we also find that this model predicts

$$\left| \frac{V_{ub}}{V_{cb}} \right| = 0.051 \pm 0.009. \quad (4.10)$$

Comparison with the measured value, 0.086 ± 0.008 , leads to a difference of 2.9σ . In Figure 1 we show the discrepancy between the experimental data and the predictions of $\sin 2\beta_{\max}$ and $|V_{ub}/V_{cb}|$ for these textures. The 2σ error bars for the experimental and predicted values do not overlap for either observable. Note, the more precise $\sin 2\beta$ measurement is slightly more effective in constraining these models than $|V_{ub}/V_{cb}|$.

We have shown in this section that even with a conservative doubling of the light quark masses listed in equation (2.2), all hierarchical texture models with $11 = 13 = 0$ and $12 = 21$ are ruled out at the 3σ level. This set includes models I, II, and IV of [13] and more general $(11 = 13 = 31 = 0)$ 4-zero texture models considered for example in GUTs.

⁵We add errors in quadrature and compare it to the difference between the central values $|\sin 2\beta_{\text{WA}} - \sin 2\beta_{\max}|$.

4.2.2 Models with non-zero 13 elements

In this section, we show that the addition of non-zero 13 elements in either Y^U or Y^D allows $\sin 2\beta$ and $|V_{ub}/V_{cb}|$ to increase enough to be consistent with the data. We choose to concentrate on two of the more constrained examples of these types of textures: models III and V listed in Table 1. We will see that these models are consistent with current data, implying that it is also true for less constrained models of this type. This result also agrees with that found by Roberts et al. [8].

The important similarities between models III and V are that both have $Y_{13}^U \neq 0$ and $Y_{12}^U = 0$. Each has 2 non-removable phases, and for both models we place one of these in Y_{13}^U . The other we place in Y_{32}^D (Y_{32}^U) for model III (V). Vanishing Y_{12}^U implies $s_{12}^U = 0$ and the CKM matrix is

$$V_{CKM} = \begin{pmatrix} 1 & s_{12}^* & s_{13}^* \\ -s_{12} & 1 & s_{23}^* \\ s_{12}^D s_{23} - s_{13} & -s_{23} - s_{12}^{D*} s_{13} & 1 \end{pmatrix}. \quad (4.11)$$

Three CKM elements are in one to one correspondence with s_{ij} . We find

$$\begin{aligned} V_{us} &= s_{12}^* = \sqrt{\frac{m_d}{m_s + m_d}}, \\ V_{ub} &= s_{13}^* = \sqrt{\frac{m_u}{m_t}} e^{-i\phi_{13}^U}, \\ V_{cb} &= s_{23}^* \end{aligned} \quad (4.12)$$

where we use equation (4.2) for $|V_{us}|$.⁶ We thus obtain predictions for V_{us} and V_{ub} in terms of quark mass ratios. The predicted values, $|V_{us}| = 0.224 \pm 0.008$ and $|V_{ub}| = 0.0031 \pm 0.0005$, agree quite well with experiment.

β is given by

$$\beta = \arg \left(\frac{1}{1 - \frac{s_{13}}{s_{12}^D s_{23}}} \right) = \arg \left(1 - \rho e^{-i\phi_{13}^U} \right) \quad (4.13)$$

where

$$\rho \equiv \left| \frac{V_{ub}}{V_{cb} V_{us}} \right|. \quad (4.14)$$

⁶For model III, the phase in Y_{32}^D enters in V_{us} through \tilde{Y}_{22}^D . However, since \tilde{Y}_{22}^D is dominated by the real Y_{22}^D , the overall phase of \tilde{Y}_{22}^D is small. Finally, since $V_{us} \simeq Y_{12}^D / \tilde{Y}_{22}^D$, this implies that V_{us} has a negligible phase.

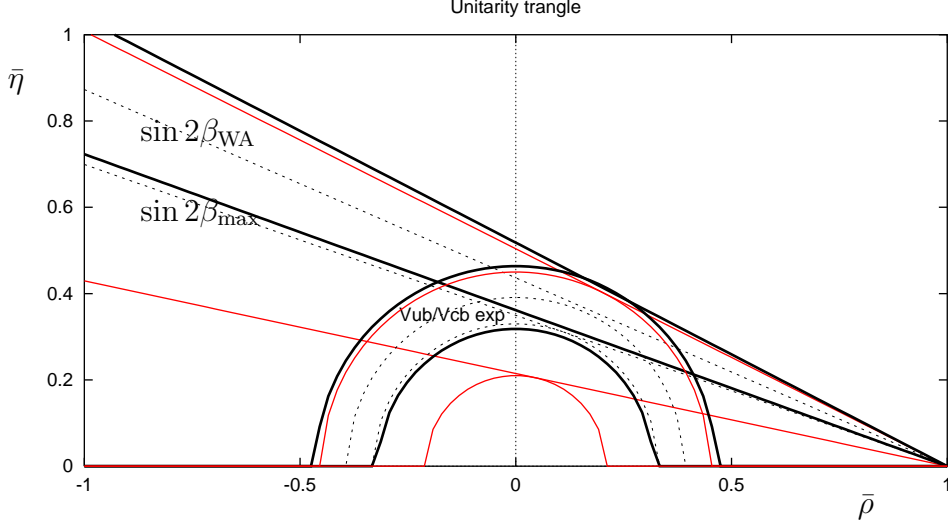


Figure 2: Comparisons between experiment and predictions of models III and V. Pictured is the predicted $\sin 2\beta_{\max}$ with red (or grey) lines for the 2σ errors and the experimental 2σ lines for $\sin 2\beta$ shown in black. Similarly, 2σ arcs are shown in red (or grey) for the predicted $|V_{ub}/V_{cb}|$, while the experimental 2σ arcs are black. There is significant overlap between the data and predicted values.

The maximum value of $\sin 2\beta$ obtained from these models is

$$\begin{aligned}\sin \beta_{\max} &= \rho = 0.33 \pm 0.06 \\ \sin 2\beta_{\max} &= 0.62 \pm 0.10.\end{aligned}\tag{4.15}$$

This value agrees with the measured $\sin 2\beta$ within 2σ . There are no further predictions to be made from models III and V.

Figure 2 compares the experimental and predicted values for models III and V. There is clearly a large amount of overlap between the predictions and experiment, showing that these two models are in agreement with current measurements. Because III and V represent rather constrained examples of a broader class of models, those models with non-zero Y_{13}^U or Y_{13}^D that have fewer texture zeros will also be consistent with the data.

5. Conclusion

In this paper we have considered hierarchical quark mass textures with symmetric $12 = 21$ and vanishing 11 elements. In Sections 4.2.1 (4.2.2) we addressed textures

with 13 = 0 ($\neq 0$) elements, respectively. In the first class of textures, $\sin \beta_{\max}$ is given by

$$r = \left| \frac{V_{ub}}{V_{cb}} \right| \sqrt{\frac{m_s}{m_d}} \approx \left| \frac{V_{ub}}{V_{cb} V_{us}} \right|, \quad (5.1)$$

while in the second class of textures $\sin \beta_{\max}$ is given by

$$\rho = \left| \frac{V_{ub}}{V_{cb} V_{us}} \right|. \quad (5.2)$$

In both cases, the maximum value of $\sin 2\beta$ is determined once $|V_{us}|$, $|V_{cb}|$ and $|V_{ub}|$ are known. The determination of $|V_{us}|$ and $|V_{cb}|$ is the same for both cases. The difference comes from the prediction for $|V_{ub}|$. For the textures with $11 = 13 = 0$ and $12 = 21$, we have $|V_{ub}/V_{cb}| = \sqrt{m_u/m_c}$. On the other hand, the second class of textures (with $13 \neq 0$) and, in particular, types III and V 5-zero textures, give $|V_{ub}| = \sqrt{m_u/m_t}$ and $|V_{ub}/V_{cb}| = \sqrt{m_u/m_c} \frac{\sqrt{m_c/m_t}}{|V_{cb}|}$. It turns out that $\frac{\sqrt{m_c/m_t}}{|V_{cb}|} \simeq 1.5$ if we take the central values of m_c , m_t and $|V_{cb}|$. As a result the hierarchical textures with $13 \neq 0$ are still consistent with the data.

We have shown that hierarchical texture zero models with $11 = 13 = 0$ and $12 = 21 \neq 0$ are ruled out at the 3σ level by measurements of $\sin 2\beta$ and $|V_{ub}/V_{cb}|$. Included in these are the 5-zero models I, II and IV of [13], and also many GUT models based on SO(10) with 4-zero textures. Allowing non-zero 13 elements alleviates the conflict, and as examples we have shown that the 5-zero models III and V of [13] predict $|V_{us}|$, $|V_{ub}|$, and $\sin 2\beta_{\max}$ values which are consistent with the data. Lastly, we expect that among the observables, $\sin 2\beta$ will become a dominant force in constraining texture zero models in the future.

Acknowledgment

We thank A. V. Manohar and A. S. Kronfeld for discussions on the quark mass error estimates.

Appendix

A. Loop Rephasing Method

The purpose of this Appendix is to present a method to easily count and place the non-removable phases of the quark mass matrices. Although Kusenko and Shrock [17]

have already given a procedure for this task, we feel that our method is in practice easier and faster to use.

For ease of reference, we present our method in a concise form here. Explanation and definitions of terms will follow.

The loop rephasing method: Form the combined quark mass matrix and find all of its loops. The number of loops in a set of basis loops is equal to the number of non-removable phases. The non-removable phases may be placed on any non-zero elements subject to the constraint that every loop has at least one corner with a phase.

A more thorough description follows, including definitions of the combined quark matrix, loops, corners, and sets of basis loops. Throughout this description we will be considering as an example model III from Table 1:

$$Y^U = \begin{pmatrix} 0 & 0 & X \\ 0 & X & 0 \\ X & 0 & X \end{pmatrix} \quad Y^D = \begin{pmatrix} 0 & X & 0 \\ X & X & X \\ 0 & X & X \end{pmatrix} \quad (\text{A.1})$$

We define the combined quark matrix \overline{Y} as the 3 by 6 matrix formed when adjoining the up and down quark matrices. The 3 rows correspond to the 3 families of $SU(2)$ doublet fields Q_i , and the 6 columns correspond to the $SU(2)$ singlet fields $(u^c, d^c)_k$.

$$Q_i \overline{Y}_{ij} \begin{pmatrix} u^c \\ d^c \end{pmatrix}_j = (Q_1, Q_2, Q_3) \begin{pmatrix} X & X & X & X & X & X \\ X & X & X & X & X & X \\ X & X & X & X & X & X \end{pmatrix} \begin{pmatrix} u_1^c \\ u_2^c \\ u_3^c \\ d_1^c \\ d_2^c \\ d_3^c \end{pmatrix} \quad (\text{A.2})$$

Although we are concerned specifically with the rephasing of combined quark matrices with three generations, the method presented here can be applied to any finite complex matrix whose fields can be rephased independently.

For model III, the combined quark matrix is

$$\overline{Y}_{\text{III}} = \begin{pmatrix} 0 & 0 & X & 0 & X & 0 \\ 0 & X & 0 & X & X & X \\ X & 0 & X & 0 & X & X \end{pmatrix} = \begin{pmatrix} 0 & 0 & Y_{13}^U & 0 & Y_{12}^D & 0 \\ 0 & Y_{22}^U & 0 & Y_{21}^D & Y_{22}^D & Y_{23}^D \\ Y_{31}^U & 0 & Y_{33}^U & 0 & Y_{32}^D & Y_{33}^D \end{pmatrix}. \quad (\text{A.3})$$

Consider horizontal and vertical lines which connect non-zero matrix elements. We define a loop to be a set of such lines which traces a closed path, provided that no two

lines are on top of one another. We further define that a corner element of a loop be an element where the loop path makes a 90° turn.

In the combined quark matrix \bar{Y}_{III} , we may form 3 loops:

$$\begin{pmatrix} 0 & 0 & \cancel{X} & \cancel{\theta} & \cancel{X} & 0 \\ 0 & X & 0 & X & X & X \\ X & 0 & \cancel{X} & \cancel{\theta} & \cancel{X} & X \end{pmatrix} \quad \begin{pmatrix} 0 & 0 & X & 0 & X & 0 \\ 0 & X & 0 & X & \cancel{X} & \cancel{X} \\ X & 0 & X & 0 & \cancel{X} & \cancel{X} \end{pmatrix} \quad \begin{pmatrix} 0 & 0 & \cancel{X} & \cancel{\theta} & \cancel{X} & 0 \\ 0 & X & 0 & X & \cancel{X} & \cancel{X} \\ X & 0 & \cancel{X} & \cancel{\theta} & \cancel{X} & \cancel{X} \end{pmatrix} \quad (\text{A.4})$$

loop₁ loop₂ loop₃

For each loop there is a corresponding rephase-invariant combination of elements. At each corner of the loop there is a non-zero matrix element. Multiply these corner elements together with the prescription that as the loop is traversed the elements should be taken as alternating with and without a complex conjugate. The phase of this product is the phase of the loop. Our convention is that we start on the left end of the upper row of the loop and take this element without a complex conjugate.

We now prove that the phase corresponding to a loop is invariant under rephasing. Consider a matrix M which contains loops. Consider further one of those loops, and further still a row (call it the i th row) which contains corners of that loop. Along this row, the corners of the loop must be connected pair-wise by horizontal lines. This follows from the definition of a loop and of loop corners. Let θ be the phase associated with the loop:

$$\theta = \arg(\dots M_{ij} M_{ik}^* \dots M_{il} M_{im}^* \dots) \quad (\text{A.5})$$

where we have shown only those corner pairs in the i th row. Rephase the i th row field by $e^{i\phi}$ so that the new matrix has the i th row elements: $M'_{ij} \equiv e^{i\phi} M_{ij}$ for all j . The phase of the loop in the new matrix will be:

$$\begin{aligned} \theta' &\equiv \arg(\dots M'_{ij} M_{ik}^* \dots M'_{il} M_{im}^* \dots) \\ &= \arg(\dots (e^{i\phi} M_{ij}) (e^{i\phi} M_{ik})^* \dots (e^{i\phi} M_{il}) (e^{i\phi} M_{im})^* \dots) \\ &= \arg(\dots M_{ij} M_{ik}^* \dots M_{il} M_{im}^* \dots) \\ &= \theta. \end{aligned} \quad (\text{A.6})$$

These same arguments clearly hold for columns as well. Therefore, rephasing any row or column cannot change θ and so the phase of the loop is a rephase-invariant quantity.

For model III the phases corresponding to the three loops are:

$$\begin{aligned} \theta_1 &= \arg(Y_{13}^U Y_{12}^{D*} Y_{32}^D Y_{33}^{U*}) \\ \theta_2 &= \arg(Y_{22}^D Y_{23}^{D*} Y_{33}^D Y_{32}^{D*}) \\ \theta_3 &= \arg(Y_{13}^U Y_{12}^{D*} Y_{22}^D Y_{23}^{D*} Y_{33}^D Y_{33}^{U*}). \end{aligned} \quad (\text{A.7})$$

Note that Y_{32}^D does not appear in the expression for θ_3 since the element does not lie on a corner of the loop.

The phases of the loops of a matrix are not necessarily independent. This can be seen in our example: $\theta_1 + \theta_2 = \theta_3$. There is a parallel between adding phases and combining loops. To add a loop, take the loop in a clockwise direction starting from the left end of the upper row of the loop. To subtract a loop, take the loop in the counter-clockwise direction starting from the same place. When adding or subtracting loops, if two loops have congruent lines with opposite directions, cancel these lines out. The resulting loop will correspond to a phase which is the sum (or difference) of phases of the input loops.

For the specific case of model III, we can see that $\text{loop}_1 + \text{loop}_2 = \text{loop}_3$:

$$\left(\begin{array}{ccccc} 0 & 0 & \overrightarrow{X-\theta} & \overrightarrow{X} & 0 \\ 0 & X & \uparrow & X & \overrightarrow{X} \\ X & 0 & \overrightarrow{X-\theta} & \overrightarrow{X} & \overrightarrow{X} \end{array} \right) \rightarrow \left(\begin{array}{ccccc} 0 & 0 & \overrightarrow{X-\theta} & \overrightarrow{X} & 0 \\ 0 & X & \uparrow & X & \overrightarrow{X} \\ X & 0 & \overrightarrow{X-\theta} & \overrightarrow{X} & \overrightarrow{X} \end{array} \right) \quad (\text{A.8})$$

We define a set of basis loops for a matrix as the minimal set of loops from which all loops of that matrix can be made by addition and subtraction. For the following, let the number of loops in a basis be equal to N . We will now prove claims relating N to the number and placement of the non-removable phases.

First, we claim that the number of phases necessary to parametrize the invariant phases of a matrix is equal to N . Our proof: Given a basis of loops for a matrix, all possible loops of that matrix can be made from linear combinations of these basis loops. Similarly, all invariant phases associated with the loops can be parametrized by the basis loop phases. As proven later in this Appendix, any loop-free matrix can be made real by rephasing. Thus all invariant phases are associated with loops, and all invariant phases in a matrix are parametrized by the N phases of the basis loops.

Our second claim is that it is always possible to place the N non-removable phases into N different elements of the matrix while choosing the rest of the matrix elements to be real. As proof we give a procedure by which we place these N phases into a configuration reachable by rephasing a matrix of complex elements. For the following, we assume $N \geq 3$. The procedure clearly works for $N = 1$ or 2 .

1) Choose any loop, then choose any corner of that loop. Place a phase on that corner and choose all other corners of that loop to be real.

2) Choose another loop, independent of the first, which does not contain the corner where we have placed the first phase.⁷ Because this loop is independent from the first,

⁷It is always possible to choose such a loop because: a) it is possible to choose a loop that is independent from the first (because $N > 1$), and b) if this second loop *did* contain the phased cor-

it must contain new corners not contained in the first loop. Among these new corners, choose one to contain a phase and choose the rest to be real.

3) Choose another loop, independent of the previous loops, which contains no phased corners. Again, it is possible to choose such a loop by combining any new, independent loop with the previous loops in such a way that we achieve a new loop which contains no previously phased corners. Once we have our desired new loop, among the new corners reached by this loop give one corner a phase and choose the rest to be real.

4) Repeat step 3) until there have been N loops chosen and N phases placed.

5) Choose as real all elements which are not corners of any loops.

Since they are independent of each other, the chosen set of loops will form a basis. Further, the set will be such that each loop in the basis has exactly one corner with a phase. This implies that each basis phase is in one to one correspondence with an arbitrary matrix element phase. Therefore, by altering these arbitrary matrix phases, we can independently alter the basis phases.

All invariant loop phases θ_i can be parametrized by these basis phases $\hat{\theta}_\alpha$:

$$\theta_i = \sum_{\alpha=1}^N a_{i\alpha} \hat{\theta}_\alpha. \quad (\text{A.9})$$

The $a_{i\alpha}$ have values ± 1 or 0 and depend only on the geometry of the matrix loops. For any given θ_i , we can alter the independent and arbitrary $\hat{\theta}_\alpha$ to give θ_i any value we choose. This implies our phase choices have resulted in a matrix in which every loop contains a corner with a phase. We show later that such a situation can be achieved by rephasing the fields of the matrix starting from arbitrary complex entries. Therefore, starting from a matrix of arbitrary complex elements, we have shown that it is possible to place the N non-removable phases in N different elements of the matrix, while making all other elements real.

In our example involving model III, any two of the loops may be considered as a basis set and so there are two non-removable phases. As a parallel, it is also clear that any two of the θ_i may combine to give the third.

Now to determine where the non-removable phases can be placed. Our claim here is that to have a correct rephasing of the matrix it is necessary and sufficient to place phases in the matrix in such a way that all loops have at least one corner with a phase. As stated above, the minimal number of phases necessary to do this is equal to N , the number of loops in a set of basis loops.

ner, we could find a third loop (independent from the first) which did not contain that corner by adding/subtracting the first and second loops.

Argument for the necessity of our claim: If after placement of phases there is a loop with no phases on corner elements, then the invariant phase corresponding to that loop is zero. However, starting from a complex matrix with arbitrary phases there is no way to rephase the fields to set an invariant phase to a specific value (zero here). Therefore, for the rephasing to be correct, each loop must have at least one corner with a phase.

Argument for the sufficiency of our claim: Let our matrix be A . Place phases in A as described above so that each loop has at least one corner with a phase. Form a new matrix B from A by setting to zero those elements where phases were just placed. By definition, B must have no loops. There exists a rephasing procedure, described below, by which all elements in a loop-free matrix such as B may be made real. The same rephasing procedure on a matrix of the form A with arbitrary phases in all elements will lead to the placement of phases we achieved by our method. Therefore, the phase placement chosen for A results in a configuration which can be achieved by rephasing a generally complex matrix A .

The rephasing procedure for a loop-free matrix is as follows. First draw all possible horizontal and vertical lines between the non-zero elements of the matrix. Define the term tree to refer to each set of connected paths. Choose a tree, and choose a row or column of the matrix which contains an element of that tree. For simplicity of language, we imagine starting with a row. For all non-zero elements in the row (all must be connected in this single tree), use the corresponding column field phases to make these elements real. Now find all other elements within the columns just used in rephasings. Note that each of these elements are connected to the previous elements by vertical lines. Because their column fields have been used already, these elements must be rephased by using their individual row fields. This is possible since no two of these elements may be in the same row, a fact which follows from the loop-free structure of the matrix and is proven later.

Now find all other elements in the rows just used. Note again that these newly found elements are connected to those just rephased by horizontal lines. Rephase these new elements by their column fields. Continue this procedure, alternating between rows and columns, until all of the elements within the tree are real.

Now we show that during our procedure, when rephasing in rows (columns), no two elements to be rephased can be in the same row (column). For simplicity, we take the case of rephasing in rows. The argument clearly also applies to columns.

Suppose that when rephasing by rows, two of the elements to be rephased lie in the same row. Because our procedure rephases elements connected by lines to those we have rephased before, any element we reach in the procedure has a path back to the original (connected) row. Our two elements we are considering are connected to each other

through two paths: the horizontal line between them, and the path which goes through the starting row of the procedure. The existence of two paths connecting two elements implies the existence of a loop in our supposed loop-free matrix. The contradiction leads us to conclude that our supposition is false. Therefore, when rephasing by rows, no two elements to be rephased will lie in the same row.

Our procedure reaches the whole tree in a finite number of steps because (by assumption) the matrix is finite which means the tree is finite, and because each step necessarily reaches more of the tree. Other trees within the matrix, by definition, have no elements on the rows or columns used by any other trees. Therefore, the trees of a matrix may be rephased independently, one after another, by the procedure described above.

As for our model III example, in section 4.2.2 we chose to place the non-removable phases in Y_{13}^U and Y_{32}^D . This places a phase on at least one corner of each loop. Removal of the elements at which we have placed phases leads us to

$$\begin{pmatrix} 0 & 0 & 0 & 0 & Y_{12}^D & 0 \\ 0 & Y_{22}^U & 0 & Y_{21}^D & Y_{22}^D & Y_{23}^D \\ Y_{31}^U & 0 & Y_{33}^U & 0 & 0 & Y_{33}^D \end{pmatrix} = \begin{pmatrix} 0 & 0 & 0 & 0 & X & 0 \\ 0 & X & \text{---} & X & X & X \\ X & \text{---} & X & \text{---} & \text{---} & X \end{pmatrix}. \quad (\text{A.10})$$

There is one tree. We now go through our rephasing procedure for which we choose to begin with the bottom row. Use columns 1, 3 and 6 to make Y_{31}^U , Y_{33}^U and Y_{33}^D real. The only other non-zero entry in these three columns is Y_{23}^D , which we rephase by row 2. In this row, there are three other non-zero entries: Y_{22}^U , Y_{21}^D and Y_{22}^D . Rephase these by columns 2, 4 and 5 respectively. There is one other element, Y_{12}^D , in these columns. Rephase it by row 1. There are no other elements in this row, and we have reached the end of the tree.

When performed on the combined quark matrix \bar{Y}_{III} starting from an arbitrary set of phases on each element, this same rephasing procedure will lead to the desired situation of having phases on only Y_{13}^U and Y_{32}^D . Note that this phase choice is not unique. For example, we could instead have placed phases on Y_{33}^U and Y_{23}^D .

References

- [1] S. Weinberg, Trans. New York Acad. Sci. **38**, 185 (1977).
- [2] F. Wilczek and A. Zee, Phys. Lett. B **70**, 418 (1977) [Erratum-ibid. **72B**, 504 (1978)].
- [3] H. Fritzsch, Phys. Lett. B **70**, 436 (1977).
- [4] M. Battaglia *et al.*, arXiv:hep-ph/0304132.

- [5] A. Hocker, H. Lacker, S. Laplace and F. Le Diberder, Eur. Phys. J. C **21**, 225 (2001) [arXiv:hep-ph/0104062]. For updated Lepton-Photon 2003 result, see: http://www.slac.stanford.edu/~laplace/ckmfitter/ckm_results_summer03.html.
- [6] R. Gupta and K. Maltman, Int. J. Mod. Phys. A **16S1B**, 591 (2001) [arXiv:hep-ph/0101132].
- [7] L. J. Hall and A. Rasin, Phys. Lett. B **315**, 164 (1993) [arXiv:hep-ph/9303303].
- [8] R. G. Roberts, A. Romanino, G. G. Ross and L. Velasco-Sevilla, Nucl. Phys. B **615**, 358 (2001) [arXiv:hep-ph/0104088].
- [9] H. Fritzsch and Z. z. Xing, Phys. Lett. B **506**, 109 (2001) [arXiv:hep-ph/0102295].
- [10] G. Raven, eConf **C0304052**, WG417 (2003) [arXiv:hep-ex/0307067].
- [11] P. Burchat *et al.*, in *Proc. of the APS/DPF/DPB Summer Study on the Future of Particle Physics (Snowmass 2001)* ed. N. Graf, eConf **C010630**, E214 (2001).
- [12] Z. Ligeti, arXiv:hep-ph/0309219.
- [13] P. Ramond, R. G. Roberts and G. G. Ross, Nucl. Phys. B **406**, 19 (1993) [arXiv:hep-ph/9303320] and references therein.
- [14] K. Hagiwara *et al.* [Particle Data Group Collaboration], Phys. Rev. D **66**, 010001 (2002).
- [15] H. Leutwyler, Phys. Lett. B **378**, 313 (1996) [arXiv:hep-ph/9602366].
- [16] C. W. Bauer, Z. Ligeti, M. Luke and A. V. Manohar, Phys. Rev. D **67**, 054012 (2003) [arXiv:hep-ph/0210027].
- [17] A. Kusenko and R. Shrock, Phys. Rev. D **50**, 30 (1994). [arXiv:hep-ph/9310307].